Coastal Dynamics 2017
Paper No. 034

WAVE HEIGHT DISTRIBUTION FOR NONLINEAR SWELL WAVES IN DEEP AND DEPTH-LIMITED WAVE CONDITIONS

Jørgen Quvang Harck Nørgaard[1], Thomas Lykke Andersen[2], and Jannie Elkær Knudsen[3]

Abstract

This paper presents initial results from an on-going study on the influence from wave nonlinearity on the wave height distribution in deep- and depth-limited nonlinear wave conditions. A fully nonlinear VOF model, IH-2VOF, is applied to model the propagation of irregular waves on a sloping sea bed from deep to shallow water, including the effects of wave breaking. Different wave nonlinearities are evaluated in the model and the effects of the wave nonlinearity, described by the so-called Ursell-number, on the wave height distributions along the sloping sea bed are evaluated. The widely used Battjes & Groenendijk (2000) shallow water wave height distribution is concluded in the present study to significantly underpredict the low-exceedance wave heights in case of very nonlinear waves. A modification of the Battjess & Groenendijk (2000) distribution is suggested in order to include the effects of wave nonlinearity.

Key words: Depth-limited wave conditions, wave nonlinearity, Ursell number, wave height distribution

1. Introduction

Reliable wave height distributions are important for engineering applications and understanding of coastal processes in shallow-water wave conditions (depth-limited wave conditions). Especially the low-exceedance wave heights are of significant importance, since these lead to the highest wave run-up and highest wave loads on coastal protection structures (such as revetments, groins, detached breakwaters etc.).

Waves are typically hind-casted or propagated from deep- to shallow-water using computationally efficient phase-averaged numerical wave models, which, however, are typically not capable of providing low-exceedance wave heights. Thus, an appropriate wave height distribution must be applied in combination with the numerical model results.

Battjes & Groenendijk (2000) suggested the widely used composite Weibull-distribution, given in Equation (1), (named *B&G-distribution* in the following) which is now recommended for use in shallow-water wave conditions in e.g. The Rock Manual (CIRIA et al., 2007) and the EurOtop Manual (Pullen et al., 2007). H_1 and H_2 are scale parameters and k_1 and k_2 are shape factors. For conditions with non-breaking waves in deep water below a certain transition wave height H_{tr}, given in Equation (2), the B&G-distribution has a shape factor k_1 =

[1]Ports, Roads and Civil Works Department, Rambøll Denmark, Prinsensgade 11, DK-9000 Aalborg, Denmark. jqhn@ramboll.dk
[2]Department of Civil Engineering, Aalborg University, Thomas Manns Vej 23, DK-9220 Aalborg Ø, Denmark. tla@civil.aau.dk
[3]Ports, Roads and Civil Works Department, Rambøll Denmark, Prinsensgade 11, DK-9000 Aalborg, Denmark. jak@ramboll.dk

2, i.e. a Rayleigh-distribution. In shallower water with depth-limited conditions the wave height distribution changes to a Weibull-distribution with a higher shape factor k_2 = 3.6.

$$F(H) = \begin{cases} 1 - \exp\left[-(H / H_1)^{k_1} \right] & \text{for} \quad H \le H_{tr} \\ 1 - \exp\left[-(H / H_2)^{k_2} \right] & \text{for} \quad H > H_{tr} \end{cases}$$
$$\left(\tilde{H}_{tr} / H_1 \right)^{k_1} = \left(\tilde{H}_{tr} / H_2 \right)^{k2} \text{ , where } \tilde{H}_{tr} = H_{tr} / H_{rms} \tag{1}$$

H_1 and H_2 are determined from the continuity constraint in Equation (1) and k_2 is calibrated against model tests. H_1 and H_2 are set to vary for varying H_{tr}. Input to the distribution is the foreshore bed slope α_f, water depth, h, and the root-mean-square wave height H_{rms} or the spectral significant wave height H_{m0}.

$$H_{tr} = (0.35 + 5.8 \tan(\alpha_f)) \cdot h \tag{2}$$

1.1 *Scope of Present Study*

Nørgaard & Lykke Andersen (2016) concluded that the deep-water Rayleigh-distribution (Longuet-Higgins, 1952) underpredicts the low-exceedance wave heights in nonlinear wave conditions. The present paper evaluates if low-exceedance wave heights are also underestimated for nonlinear waves in depth-limited conditions. The performance of the B&G-distribution is evaluated against wave height distributions for highly nonlinear depth-limited wave conditions modelled in the three-dimensional VOF wave propagation model IH2VOF.

2. Recent Developments on the Influence from Wave Nonlinearity on Wave Height Distributions in Deep Water

Nørgaard & Lykke Andersen (2016) evaluated the deep water wave height distribution (Rayleigh-distribution) by Longuet-Higgins (1952), given in Equation (3), against highly nonlinear waves simulated in the numerical Boussinesq model MIKE21 BW by DHI. The model was validated against physical model tests performed at Aalborg University, Denmark, and against the VOF-model; IH2VOF, developed at IH-Cantabria, Spain. $H_{1/3}$ in Equation (3) is the significant wave height in the time domain.

$$F(H) = 1 - \exp\left(-2 \left(\frac{H}{H_{1/3}} \right)^b \right), \text{ where } b = 2 \tag{3}$$

Based on the study by Nørgaard & Lykke Andersen (2016) it was concluded, that the wave height distributions of highly nonlinear waves (mainly swells) was indeed influenced by wave nonlinearity, and the Rayleigh-distribution therefore significantly underestimated the low-exceedance waves in such conditions. Thus, Nørgaard & Lykke Andersen (2016) fitted the shape factor, b, in the Rayleigh-distribution to the so-called Ursell-number, given in Equation (4), which was shown to be a suitable parameter for description of the influence from nonlinear waves.

High values of U_r indicate long waves with finite-amplitude in shallow water that necessitate the use of nonlinear wave theory. As seen from Figure 1 the Stokes 2nd order wave theory is applicable up to U_r=26. For irregular waves Nørgaard & Lykke Andersen (2016) concluded that H_{m0} (significant wave height based on the frequency domain) and $L_{0.1}$ (wave length corresponding to the local $T_{0.1}$ based on the linear dispersion relation) was the best descriptors for H and L in Equation (4).

$$U_r(H,L) = \frac{H/h}{(h/L)^2} = \frac{\text{"Nonlinearity" (measure of wave height)}}{\text{"Shallowness" (measure of depth/length)}} \tag{4}$$

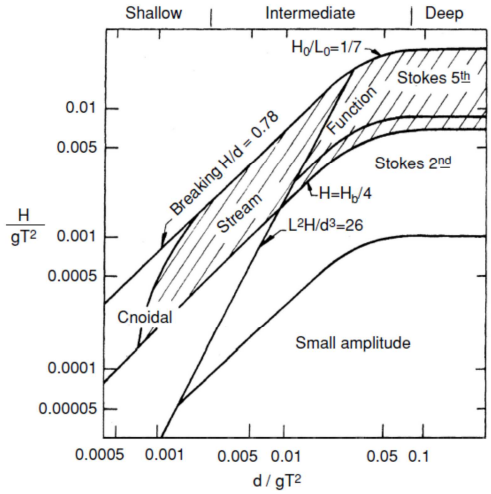

Figure 1: Diagram by Le Mehaute (1969) for validity of different wave theories.

Examples are given in Figure 2 for two different nonlinearities (U_r=0.05 and U_r=369) described by the Stokes linear wave theory and the Stream Function theory, respectively.

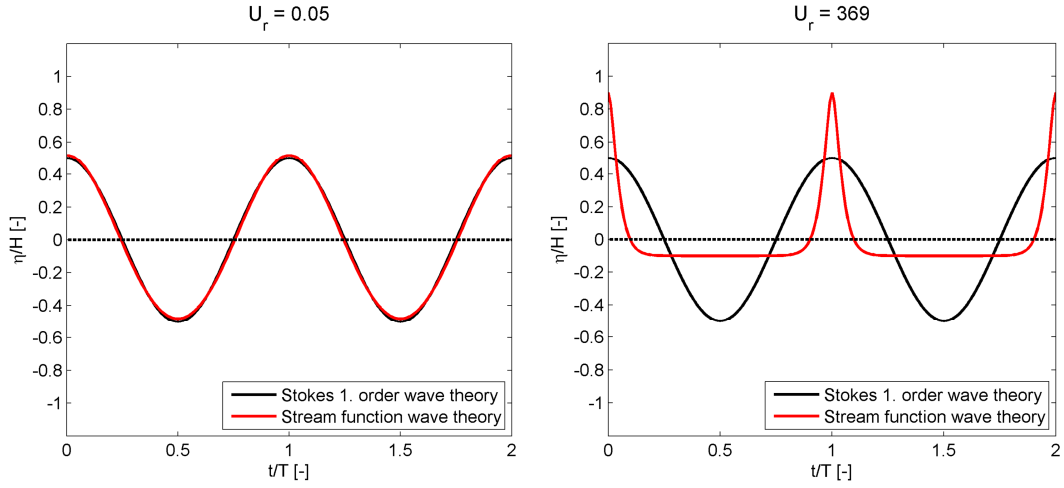

Figure 2: *(left)* Surface elevations of linear waves (U_r=0.05) *(right)* Surface elevations of nonlinear waves (U_r=369).

In addition to $U_r(H_{m0},L_{0.1})$ also various slopes (1:30 – 1:100) and two different so-called peak-enhancement factors in the JONSWAP spectra (γ=3.3 and γ=10) was evaluated by Nørgaard & Lykke Andersen (2016). It was concluded, that the modified wave height distribution in Equation (5) with the fitted shape factor, *b*, was performing very well in the prediction of the wave height distribution for linear to highly nonlinear non-breaking waves (i.e. $H_{m0}/h \leq 0.2$).

$$F(H) = 1 - \exp\left(-a\left(\frac{H}{H_{1/3}} \right)^b \right)$$
$$where\ a = 2,\ b = \begin{cases} 2 & \text{for } U_r(H_{m0},L_{0.1}) \leq 26 \\ -0.00582 \cdot U_r(H_{m0},L_{0.1}) + 2.151 & \text{for } 26 < U_r(H_{m0},L_{0.1}) \leq 105 \end{cases} \quad (5)$$

The influence from $U_r(H_{m0},L_{0.1})$ on the ratios $H_{1/3}/H_{m0}$ (given in Equation (6)) and $T_{0.1}/T_p$ (given in Equation (7)) was further investigated by Nørgaard & Lykke Andersen (2016) for use in the transformation of the input wave parameters for Equation (5).

$$\frac{H_{1/3}}{H_{m0}} = a \cdot U_r\left(H_{m0},L_{0.1,deep}\right) + 0.97 \qquad \text{for } \alpha < U_r(H_{m0},L_{0.1,deep}) \leq \beta$$
$$where: \quad (6)$$
$$a = 0.0008 \text{ for slope=1:30 and } \alpha = 0,\ \beta = 190$$

$$\frac{T_{0.1}}{T_p} = C_\gamma\left(a \cdot U_r(H_{m0},L_p) + b\right) + 0.97 \qquad \text{for } \alpha < U_r(H_{m0},L_p) \leq \beta$$
$$where: \quad (7)$$
$$C_\gamma = 0.939,\ a = 0,\ b = 0 \text{ for slope=1:30 and } \alpha = 0,\ \beta = 20$$
$$C_\gamma = 0.939,\ a = -0.0008,\ b = 0.871 \text{ for slope=1:30 and } \alpha = 20,\ \beta = 190.6$$

3. Evaluation on the Influence from Wave Nonlinearity on Wave Height Distributions in Depth Limited Conditions

The nonlinear waves are in the present study solely modelled with a single peak enhancement factor, γ=10, corresponding to swell waves, and a single sea bed slope, 1:30. However, different wave periods, different $U_r(H_{m0},L_{0.1})$, and different ratios of H_{m0}/h are considered, meaning that both intermediate to shallow water and mildly to highly nonlinear waves are evaluated. Additionally, a single case with relatively linear waves is evaluated using γ=3.3, which is used for validation of the model setup.

The investigation of the wave height distributions for nonlinear irregular waves using physical model tests requires large laboratory facilities (long wave flumes) since a sufficient water depth is required at the wave generation paddle in order to avoid the generation of spurious waves when applying 2. order irregular wave generation, cf. Figure 1. Therefore, the highly sophisticated IH-2VOF model, developed by IH-Cantabria, Spain, is applied for the present study. The model and the model setup for the present study are described in the following.

3.1 *Description of Numerical Model and Model Setup*

IH-2VOF solves the two-dimensional Reynolds Averaged Navier-Stokes (RANS) equations and is capable of simulating all important wave transformation processes, which are considered in the present study, such as wave shoaling, wave breaking, and nonlinear wave-wave interactions. The model is extensively validated in several studies, such as Torres-Freyermuth et al. (2007), Torres-Freyermuth et al. (2010) and Lara et al. (2011).

The applied numerical wave flume for the present study in IH-2VOF is illustrated in Figure 3. The water depth at the wave generation boundary (left side of the flume in Figure 3) is chosen to be sufficiently deep in order to fulfil the requirements given in Figure 1. The sea bed slope is 1:30 and the sea bed is impermeable. Waves are fully absorbed at both the left and right side of the flume. The applied mesh discretization in the model is based on convergence analysis and the recommendations given in the IH-2VOF manual.

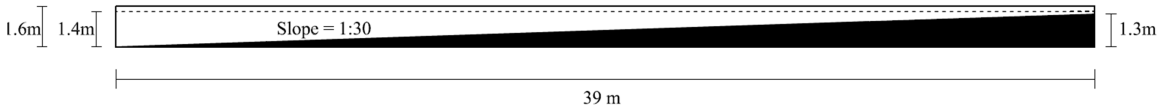

Figure 3: Applied model domain in IH-2VOF in the present study.

JONSWAP spectra are generated in the flume using 2. order irregular wave generation theory and surface elevations are obtained at multiple positions along the flume (positioned with spacing's of 1 m along the flume). In this way each model simulation results in several wave height distributions along the flume with varying $U_r(H_{m0},L_{0.1})$. 1000 waves are considered in each model simulation.

Before applying the IH-2VOF model in the evaluation of nonlinear waves a validation of the model is performed by comparing results from linear deep- and depth-limited wave conditions against the Rayleigh-distribution and the B&G-distribution.

3.2 *Validation of IH-2VOF in Linear Deep and Depth-Limited Wave Conditions*

Input wave conditions for the validation of IH-2VOF in linear wave conditions are:

- **Simulation 1:** H_{m0}=0.15 m, T_p=1.5 s, γ=3.3 (JONSWAP-spectra – 2. order irregular wave generation)

Figure 4 shows the comparison of measured wave heights (simulated in IH-2VOF) against the Rayleigh-distribution and the B&G-distribution in linear deep water wave conditions (Simulation 1). The wave analysis from the surface elevation is performed using WaveLab, developed at Aalborg University, Denmark. As seen, the Rayleigh distribution and the B&G-distribution provide very similar results. A small deviation is obtained since the Rayleigh-distribution is based on the mean wave height, H_m, and the B&G-distribution is based on H_{mo} in the present case. The deviation is considered to be within the natural variation of wave parameters.

As seen from Figure 4 IH-2VOF is capable of simulating Rayleigh-distributed waves at the deep water boundary.

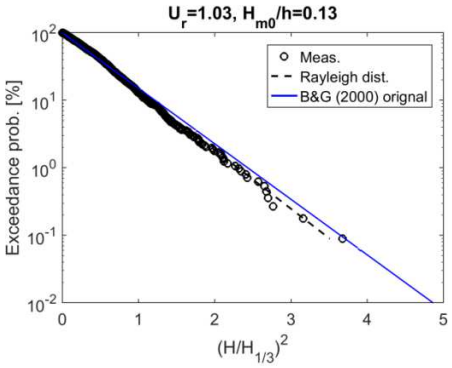

Figure 4: Comparison of simulated waves at relatively deep water against the Rayleigh distribution and the B&G-distribution in Simulation 1.

Figure 5 shows the modelled wave spectra and the target JONSWAP wave spectra corresponding to the same wave conditions as presented in Figure 4. As seen the modelled wave spectra is in accordance to the target JONSWAP wave spectra.

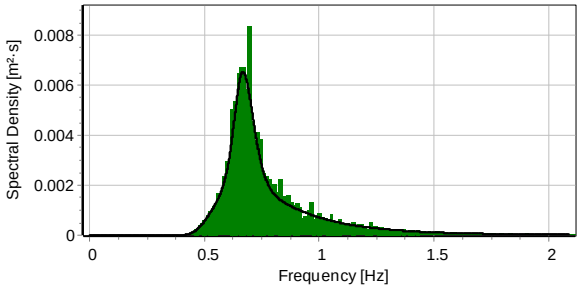

Figure 5: Modelled wave spectrum and target JONSWAP wave spectrum corresponding to the same conditions as presented in Figure 4 (Simulation 1).

Figure 6 shows the comparison of measured wave heights (simulated in IH-2VOF) against the Rayleigh-distribution and the B&G-distribution in relatively linear (Simulation 1) depth-limited wave conditions $U_r(H_{m0},L_{0.1})$, where the waves are shoaled onto 0.3 m water depth. As seen, the simulated wave heights are very much in correspondence with the predictions by the B&G-distribution, whereas, as expected, the Rayleigh distribution significantly overestimates the low-exceedance wave heights.

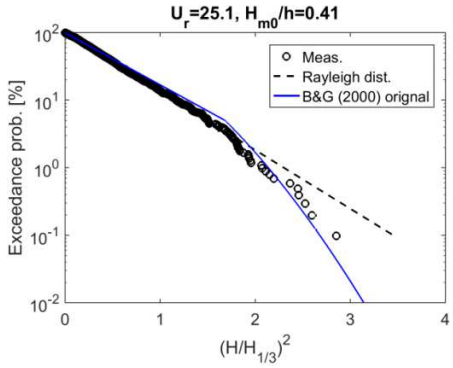

Figure 6: Comparison of simulated waves at shallow water against the Rayleigh distribution and the B&G-distribution in Simulation 1.

Figure 7 shows the modelled wave spectra and the input JONSWAP wave spectra corresponding to the same wave conditions as presented in Figure 6. As seen, both sub- and super harmonics of 2. order starts to develop and energy is dissipated due to wave breaking (compared to Figure 5).

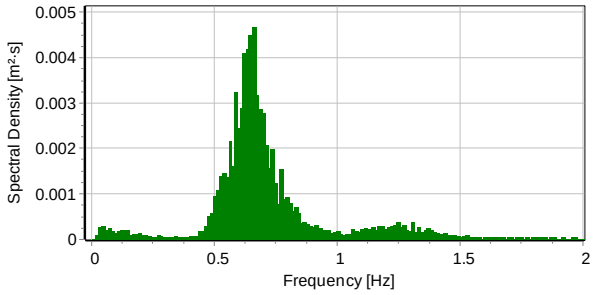

Figure 7: Modelled wave spectrum corresponding to the same conditions as presented in Figure 6 (Simulation 1).

3.3 *Simulation of Intermediate to Highly Nonlinear Depth-Limited Waves*

Due to the relatively time-consuming model simulations in IH-2VOF solely two simulations are considered in the following evaluation on the influence from wave nonlinearity on the wave height distribution in depth-limited conditions. The following JONSWAP input wave parameters are evaluated:

- **Simulation 2**: H_{m0}=0.1 m, T_p=4 s, γ=10 (JONSWAP-spectra – 2. order irregular wave generation)
- **Simulation 3**: H_{m0}=0.1 m, T_p=5 s, γ=10 (JONSWAP-spectra – 2. order irregular wave generation)

As an example, Figure 8 shows the modelled wave spectra and the input wave spectra for Simulation 2 at the deep water boundary of the wave flume.

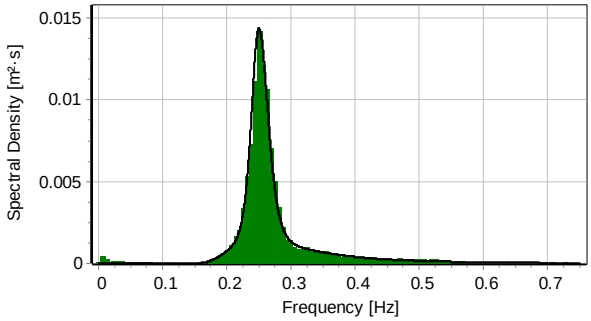

Figure 8: Modelled wave spectrum and target JONSWAP wave spectrum (Simulation 2).

Figure 9 shows a comparison between the measured (simulated) wave heights against the B&G-distribution in depth-limited highly nonlinear wave conditions for Simulation 2. As seen, the B&G-distribution significantly underestimates the low-exceedance wave heights. The tendency is that the simulated nonlinear waves starts to break much later (at higher H_{tr}) compared to the predicted H_{tr} by the B&G-distribution.

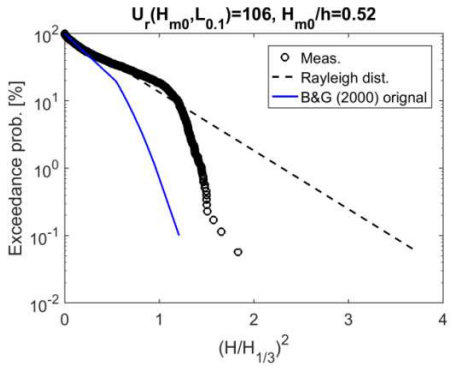

Figure 9: Example case with comparison of simulated nonlinear waves at shallow water against the Rayleigh distribution and the B&G-distribution in Simulation 2.

Figure 10 shows the modelled wave spectra for the same conditions as presented in Figure 9. As seen, the wave spectra shows highly nonlinear conditions with energy re-distributed to the sub- and superharmonics.

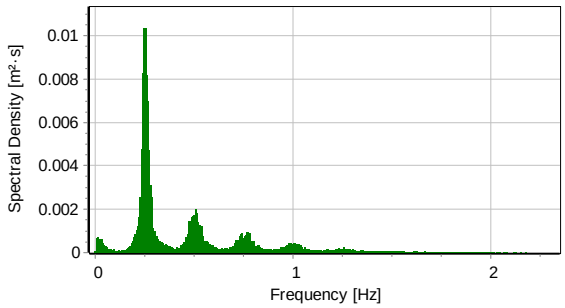

Figure 10: Modelled wave spectrum corresponding to the same conditions as presented in Figure 9 (Simulation 2).

Figure 11 shows ratios of $H_{\alpha,meas.}/H_{\alpha,pred.}$ for different exceedance probabilities; α=0.1%, α=1%, α=2%, α=5%, α=10%. $H_{\alpha,pred.}$ are obtained from the B&G-distribution in Equation (1). The ratios are obtained from the linear conditions in Simulation 1 and the nonlinear conditions in Simulation 2, and 3. Solely conditions where $H_{tr}<H_{0.1\%}$ are considered in Figure 11. As seen, the tendency is that the B&G-distribution is under-predicting the low-exceedance wave heights for increasing $U_r(H_{m0},L_{0.1})$ by up to approximately 40%, which was also expected based on the comparisons in Figure 6 and Figure 9, whereas they are well predicted for $U_r \leq 26$.

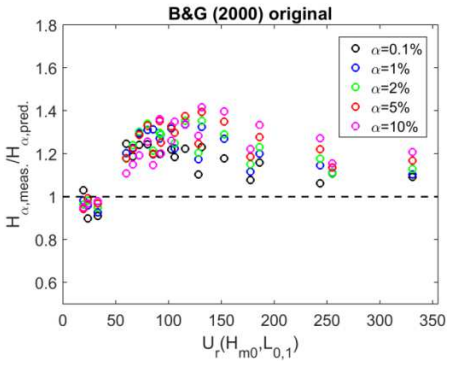

Figure 11: Comparison of simulated nonlinear waves at shallow water against the B&G-distribution in Equation (1).

4. Suggestions for Modification of the B&G-distribution to Include the Effects of Wave Nonlinearity

In order to apply the fitted shape factor by Nørgaard & Lykke Andersen (2016) in the present study (i.e. to reuse k_1 in the Rayleigh distribution), the part of the B&G-distribution, which represents the deep water wave conditions, is in the following suggested to be based on $H_{1/3}$ instead of H_{rms} as the original distribution in Equation (1). Note that Equation (5) is extended to be valid for $U_r(H_{m0},L_{0.1}) \leq 330$. Additionally, it is suggested to include a correction factor C_{tr} for modification of H_{tr} as function of $U_r(H_{m0},L_{0.1})$ as it was previously found in Figure 9 that H_{tr} was underestimated. The new suggested B&G distribution is given in Equation (8). The correction factor C_{tr} will be calibrated in the following. Note that Equation (8) is providing similar results to Equation (1) in case of $U_r(H_{m0},L_{0.1}) \leq 26$.

$$F(H)=\begin{cases}1-\exp\left[-a\cdot(H/H_{1/3})^{k_1(U_r)}\right] & \text{for } H\leq H_{tr}\\ 1-\exp\left[-a\cdot(H/H_2)^{k_2}\right] & \text{for } H>H_{tr}\end{cases}, \text{ where:}$$

$$a=2,\ k_2=3.6,\ k_1(U_r)=\begin{cases}2 & \text{for } U_r(H_{m0},L_{0.1})\leq 26\\ -0.00582\cdot U_r(H_{m0},L_{0.1})+2.151 & \text{for } 26<U_r(H_{m0},L_{0.1})\leq 330\end{cases} \quad (8)$$

$$H_{tr}=(0.35+5.8\tan(\alpha_f))\cdot h\cdot C_{tr}(U_r)$$

$$\left(\tilde{H}_{tr}\right)^{k_1(U_r)}=\left(\tilde{H}_{tr}/H_2\right)^{k_2},\ \text{where } \tilde{H}_{tr}=H_{tr}/H_{1/3}$$

4.1 *Modification of H_{tr} to Include the Effects of Wave Nonlinearity*

The influence of wave nonlinearity on the ratios $H_{tr,meas.}/H_{tr,pred.}$ is shown in Figure 12 where $H_{tr,pred.}$ is obtained based on Equation (8) with the modified k_1 shape factor by Nørgaard & Lykke Andersen (2016), however, where initially C_{tr}=1. Solely conditions where $H_{tr}<H_{0.1\%}$ are considered in Figure 12.

$H_{tr,meas.}$ is obtained from visual inspection of the different modelled wave height distributions by detecting the translation position from the relatively Rayleigh-distributed waves to the Weibull distributed waves.

As seen in Figure 12, the tendency is that H_{tr} starts to increase for $26 \leq U_r(H_{m0},L_{0.1})$ to reach a constant level of $C_{tr} = H_{tr,meas.}/H_{tr,pred.} = 1.52$ for $U_r(H_{m0},L_{0.1})>180$. The power curve in Equation (9) is fitted to the ratios in Figure 12 (the dashed line).

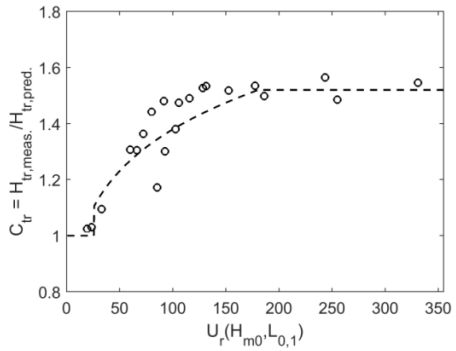

Figure 12: Influence of wave nonlinearity on H_{tr} and fitted correction factor for C_{tr} given in Equation (9).

$$C_{tr}(U_r) = \begin{cases} 1.00 & \text{for } U_r(H_{m0},L_{0.1}) \leq 26 \\ 0.65 \cdot U_r(H_{m0},L_{0.1})^{0.165} & \text{for } 26 < U_r(H_{m0},L_{0.1}) \leq 180 \\ 1.52 & \text{for } 180 < U_r(H_{m0},L_{0.1}) \leq 330 \end{cases} \quad (9)$$

A similar plot to Figure 11 is shown in Figure 13 where the correction factor in Equation (9) is included in Equation (8) for modification of H_{tr}. Solely conditions where $H_{tr}<H_{0.1\%}$ are considered in Figure 13. As seen, the modified wave height distribution provides a much safer estimate for the low exceedance wave heights in case of high wave nonlinearity (high $U_r(H_{m0},L_{0.1})$) compared to the original B&G-distribution in Equation (1).

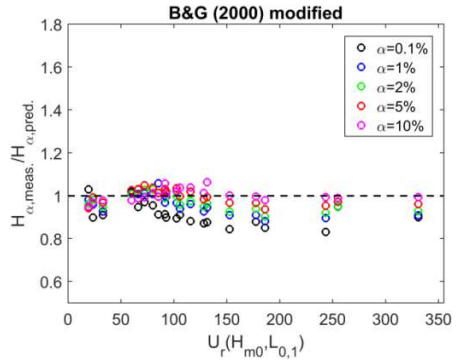

Figure 13: Comparison of simulated nonlinear waves at shallow water against the modified B&G-distribution in Equation (8) using the modification factor in Equation (9).

An example case on the performance of the modified B&G-distribution is shown in Figure 14.

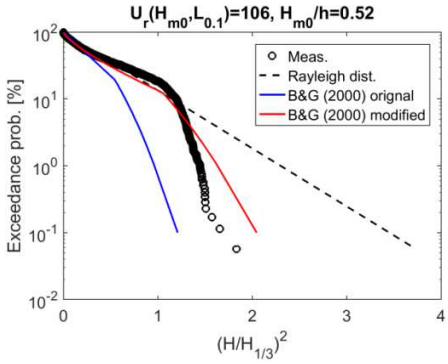

Figure 14: Example case with comparison of simulated nonlinear waves at shallow water against the Rayleigh-distribution, the original B&G-distribution in Equation (1), and the modified B&G-distribution in Equation (8).

The lowest evaluated exceedance probabilities, α = 0.1% - 2%, are slightly overestimated in the modified B&G-distribution c.f. Figure 13 and Figure 14, which indicates that the influence from the wave nonlinearity on k_2 should be further clarified. However, a bigger data foundation is needed for such study. Moreover, additional model tests are needed for clarification on the influence from the peak enhancement factor γ in the JONSWAP spectra and the bed slope on both H_{tr} and k_2.

5. Conclusions and Discussion of Findings

Initial modifications are made to include the effects of wave nonlinearity on the wave height distribution by Battjess & Groenendijk (2000). The wave nonlinearity is concluded to have significant effect on the so-called transition wave height, which defines the transition between deep- and shallow water wave conditions. Nonlinear waves seems to break in shallower water compared to linear wave conditions, which results in underpredictions of the low-exceedance wave heights by the original B&G distribution (unsafe).

Figure 15 presents an example case on the ratio between $H_{B\&G\ mod.0.1\%}$ obtained from the modified B&G-distribution in Equation (8) and $H_{B\&G\ orig.0.1\%}$ obtained from the original B&G-distribution in Equation (1) for varying $T_{0.1}$ and H_{m0} in 10 m water depth on slope 1:30 (i.e. for varying wave nonlinearities). As seen, the original B&G-distribution provide $H_{0.1\%}$ which are up to 30 – 40% lower compared to the modified wave height distribution including the suggestions for introducing wave nonlinearity in the present paper.

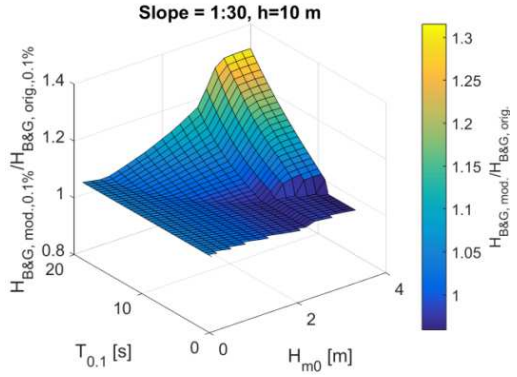

Figure 15: Example case on the influence from wave nonlinearity on the ratio between $H_{0.1\%}$ obtained from the modified B&G-distribution and the original B&G-distribution.

5.1 *Suggestions for Further Investigations*

The authors of the present paper are continuously working on refining the wave height distributions and to provide safe and easily applied tools for prediction of low-exceedance wave heights in deep- to depth-limited linear to nonlinear wave conditions. This includes further evaluation of the influence from U_r on the ratios $H_{1/3}/H_{m0}$ and $T_{0.1}/T_p$, which are needed in the conversion between wave input parameters for Equation (8) and (9). Moreover, additional sea bed slopes and peak enhancement factors will be evaluated in the future together with the influence from U_r on the shape factor, k_2, in the Weibull-distribution.

The present study solely focus on long-crested waves, which however, is also the most relevant in case of very long waves in relatively shallow water since these are typically swell and are already refracted when the waves are propagated to shallower water. Thereby they naturally only include very little directional spreading. No extra effort on the influence from 3D waves is therefore planned in on-going investigations.

References

Battjes, J.A., and Groenendijk H.W. 2000. Wave height distributions on shallow foreshores, *Coastal Engineering*, 40, 161-182. 34-550, New York.

CIRIA, CUR, CETMEF, 2007. *The Rock Manual: The Use of Rock in Hydraulic Engineering*. 2nd edition. CIRIA, London.

Lara, J.L., Ruju, A., Losada, I.J., 2011. RANS modelling of long waves induced by a transient wave group on a beach. *Proc. R. Soc.* A 467, 1215–1242.

Le Mehaute, B., 1969. An Introduction to Hydrodynamics and Water Waves, *Water Wave Theories.* Vol. II. U.S. Department of Commerce, ESSA, Washington, DC (TR ERL 118-POL-3-2).

Longuet-Higgins, M. S. (1952). On the Statistical Distribution of the Heights of Sea Waves. *Journal of Marine Research*, 11(3), PP. 245-266.

Nørgaard, J. H., & Andersen, T. L. (2016). Can the Rayleigh distribution be used to determine extreme wave heights in non-breaking swell conditions? *Coastal Engineering*, 111(May), 50-59. DOI: 10.1016/j.coastaleng.2016.01.010

Pullen, T., Allsop, W., Bruce, T., Kortenhaus, A., Schuttrumpf, H. & van der Meer, J. (2007). *Wave overtopping of sea defenses and related structure:* Assessment manual. www.overtopping-manual.com

Torres-Freyermuth, A., Losada, I.J., Lara, J.L., 2007. Modeling of surf zone processes on a natural beach using Reynolds-Averaged Navier–Stokes equations. *J. Geophys. Res. Oceans AGU*. (Am. Geophys. Union) 112, C09014.

Torres-Freyermuth, A., Lara, J.L., *Losada, I.J., 2010. Numerical modelling of short- and longwave transformation on a barred beach. Coast*. Eng., ELSEVIER 57 (3), 317–330.